^{18}O Isotope Exchange Measurements Reveal that Calcium Is Involved in the Binding of One Substrate-Water Molecule to the Oxygen-Evolving Complex in Photosystem II

Garth Hendry and Tom Wydrzynski*

Photobioenergetics, Research School of Biological Sciences, The Australian National University, Canberra ACT 0200, Australia

Received February 18, 2003; Revised Manuscript Received April 1, 2003

ABSTRACT: Direct evidence is presented to show that calcium is inherently involved in the binding of one of the two substrate-water molecules to the oxygen-evolving complex in photosystem II. Previous rapid (millisecond range) ^{18}O isotope exchange measurements between added $H_2{}^{18}O$ and the photogenerated O_2 have shown that the two substrate−water molecules bind to separate sites throughout the S-state cycle, as revealed by their kinetically distinct rates of ^{18}O exchange [Hillier, W., and Wydrzynski, T. (2000) *Biochemistry 39*, 4399−4405]. Upon extraction of the functionally bound calcium using a either a low-pH/citrate treatment or a NaCl/A23187/EGTA treatment and subsequent reconstitution of activity with strontium, we show for the first time a specific increase in the slow rate of ^{18}O exchange by a factor of 3−4. This increase in the slow rate of exchange is consistently observed across the S_1, S_2, and S_3 states. In contrast, the fast phase of ^{18}O exchange in the S_3 state appears to be affected little upon strontium reconstitution, while the fast phases of exchange in the S_1 and S_2 states remain largely unresolvable, at the detectable limits of the current techniques. The results are discussed in terms of a possible substrate bridging structure between the functional calcium and a catalytic manganese ion that gives rise to the slowly exchanging component.

Water oxidation in photosynthesis occurs in a special pigment−protein complex called photosystem II (PSII)[1] and is catalyzed by a cluster of four manganese ions (Mn_4) and a redox-active tyrosine (Y_Z) [for extensive reviews, see the special issue on photosynthetic water oxidation of *Biochimica et Biophysica Acta* (2001) *1503*, 1−259]. Collectively, the catalytic domain is known as the oxygen-evolving complex (OEC). The OEC reaction sequence proceeds through a series of four light-driven, one-electron oxidation steps, which begins from an initial "S_0" state and advances through to a metastable "S_4" state. Once S_4 has been reached, O_2 is released within 1−2 ms, the S_0 state is regenerated, and the reaction sequence begins anew. In dark-adapted samples, the OEC relaxes to the stable S_1 state (*1*, *2*).

Calcium is known to be an essential cofactor for photosynthetic water oxidation (*3*, *4*). The number of intrinsic Ca^{2+} sites in PSII has been determined using a variety of experimental approaches (*5*−*10*). It is generally agreed that there are two physiologically important Ca^{2+}-binding sites per PSII reaction center: a high-affinity site located within the light-harvesting array and a low-affinity site located within the OEC. Selective removal of Ca^{2+} from the low-affinity OEC site abolishes the O_2 evolving activity, which can be largely restored by the re-addition of Ca^{2+} (10−20 mM) or, to a lesser extent, of Sr^{2+} (*11*−*13*). It has been shown that Sr^{2+} reactivates the same number of O_2-evolving centers as Ca^{2+}, but results in a slower turnover of the reaction sequence (*13*−*15*). The release of the functional Ca^{2+} from the OEC is facilitated by the removal of the 17 and 23 kDa extrinsic proteins (*16*, *17*), suggesting that these proteins modulate the affinity of the Ca^{2+} binding site (*18*, *19*).

Substitution with other metal cations at the Ca^{2+} site has been used in attempt to elucidate the role of Ca^{2+} in O_2 evolution. Two main factors seem to determine the metal cation selectivity of the Ca^{2+} site: (1) the size of the binding cavity and (2) the negative charge density of the ligand array (*18*). Using steady-state enzyme kinetic analysis, Vrettos et al. (*18*) examined the reversible inhibition of O_2 evolution by a series of mono-, di-, and trivalent metal cations. Their results indicated that the Ca^{2+} site is highly size selective and that only divalent and trivalent metal cations of similar ionic radii to Ca^{2+} could compete at the Ca^{2+} site. On the other hand, monovalent cations with a smaller ionic radius, such as Na^+, appear to be unable to bind to the Ca^{2+} site due to its high negative charge density. In contrast, Ono et al. (*20*) found that O_2 evolution could be competitively inhibited by monovalent cations such as K^+, Rb^+, and Cs^+, which have larger ionic radii than Ca^{2+}. By using thermoluminescence and S_2-state, Mn-multiline EPR measurements, the authors provided evidence to show that the Ca^{2+} site can indeed be occupied by K^+, Rb^+, and Cs^+. Interestingly, under these conditions, the protein structure in the vicinity of the Mn_4 cluster is significantly perturbed (*21*).

* To whom correspondence should be addressed. E-mail: TOM@rsbs.anu.edu.au. Telephone: +61 (02) 6125 5892. Fax: +61 (02) 6125 8056.

[1] Abbreviations: Chl, chlorophyll; OEC, oxygen-evolving complex; PSII, photosystem II.

10.1021/bi034279i CCC: $25.00
Published on Web 05/02/2003

Perturbations to the Ca^{2+} site are known to modify the redox and magnetic properties of the OEC. For example, PSII preparations reconstituted with Sr^{2+} produce the so-called S_2-state, split EPR signal at $g = 4.1$, which is concomitant with a decrease and modification of the S_2-state, Mn-multiline EPR signal at $g = 2$ (*13*). In contrast, for Ca^{2+}-depleted preparations, redox transitions beyond the S_2 state are blocked and result in the formation of different EPR signals. In particular, the Mn-multiline signal under this condition was found to be stable for long periods of time (hours) at room temperature and to exhibit narrower ^{55}Mn hyperfine splittings (*22*−*24*). Interestingly, formation of this Mn-multiline signal was found to be dependent on the presence of the chelators used during the Ca^{2+} depletion procedure (e.g., citrate, EGTA, and EDTA) (*24*, *25*). Upon further illumination of Ca^{2+}-depleted samples at 277 K, a broad signal centered at $g = 2$ appears. The organic radical responsible for this signal was initially identified as an oxidized histidine (*26*, *27*). However, on the basis of ENDOR and ESEEM measurements, it was suggested that the radical signal arises from interactions with Y_Z^{ox} (*28*−*31*).

The recent 3.7−3.8 Å X-ray crystal structures of PSII from *Thermosynechococcus elongatus* (*32*, *33*) have identified the position, size, and shape of the Mn_4 cluster involved in O_2 evolution. However, it has not provided any details about the location of the Ca^{2+} site. Nevertheless, there is mounting evidence that Ca^{2+} is in the proximity of the Mn_4 cluster. Substitution of the Ca^{2+} site with Mn^{2+} results in a strong enhancement in the spin relaxation of S_2-state, Mn-multiline EPR signals (*34*). NMR studies after substitution of the Ca^{2+} site with $^{113}Cd^{2+}$ indicate that the binding pocket consists of a symmetrical, six-coordinate sphere containing oxygen, nitrogen, and chlorine ligands (*35*). Mn EXAFS measurements have indicated a significant interaction of Ca^{2+} (Sr^{2+}) with the Mn_4 cluster at ∼3.3 Å (*36*, *37*), in which this interaction is strongly inhibited upon Ca^{2+} depletion (ref *38* and reviewed in ref *39*). It has been suggested that Ca^{2+} is ligated to the Mn_4 cluster via a carboxylate bridge (*40*). Support for this idea originally came from FTIR difference spectroscopy, in which certain COO^- stretching modes were associated with Ca^{2+} interactions (*41*); however, the same modes have also been interpreted in terms of chelator interactions with the catalytic site (*20*).

A number of different roles have been proposed for Ca^{2+} in the water oxidation mechanism. Early suggestions implied that Ca^{2+} optimizes the structure of the catalytic site (*3*, *42*), through the regulation of electrostatic constraints (*14*) or by providing a docking site for the Cl^- cofactor (*43*, *44*). Ca^{2+} has also been suggested to play a "gatekeeper" role by controlling solvent water access (*19*, *23*). However, it has been argued that if the role of Ca^{2+} were purely structural in nature, then other metal cations with similar ionic properties would be able to restore at least some activity in Ca^{2+}-depleted preparations, whereas only Sr^{2+} can functionally replace Ca^{2+} (*18*, *20*). Thus, it has been proposed that Ca^{2+} plays a direct role in photosynthetic water oxidation, in particular, by acting as a binding site for the substrate water (*43*, *45*−*49*).

To address the role of Ca^{2+} in photosynthetic water oxidation, we have undertaken kinetic measurements of ^{18}O exchange in PSII samples following replacement of the functional Ca^{2+} with Sr^{2+}. Using special time-resolved mass spectrometric techniques that kinetically distinguish the binding of the two substrate-water molecules to the OEC, we present the first evidence that Ca^{2+} directly interacts with the binding for one of the two substrate-water molecules.

EXPERIMENTAL PROCEDURES

Sample Preparation. PSII-enriched membrane fragments were isolated from fresh market spinach according to the procedure of Berthold et al. (*50*). Briefly, thylakoid membranes were solubilized in 5% Triton X-100 buffered in 30 mM MES/NaOH (pH 6.3), 15 mM NaCl, and 5 mM $MgCl_2$, by gentle stirring for 20 min in the dark at 4 °C. The PSII samples were collected by centrifugation for 20 min at 36000*g* and 4 °C and were washed and resuspended in a standard buffer medium consisting of 30 mM MES/NaOH (pH 6.3), 15 mM NaCl, 5 mM $MgCl_2$, and 400 mM sucrose. The PSII-enriched membranes were then snap-frozen in liquid N_2 at a density of 2−4 mg of Chl/mL and stored at −80 °C until they were used.

Calcium Depletion. Acid-induced depletion of the functional Ca^{2+} from the OEC was performed using a low-pH/citrate treatment (*36*, *51*). Samples treated in this manner are called "Ca^{2+}-depleted". PSII-enriched membranes were first washed in 0.25 mM MES/NaOH (pH 6.3), 15 mM NaCl, and 400 mM sucrose and suspended to a density of 4 mg of Chl/mL. They were then diluted with an equal volume of a citrate buffer medium containing 20 mM citrate (pH 3.0), 15 mM NaCl, and 400 mM sucrose and allowed to incubate at 0 °C for 5 min with gentle stirring. After incubation, the sample was rapidly brought to physiological pH by diluting it (1:2) with a buffer medium consisting of 50 mM MES/NaOH (pH 6.3), 15 mM NaCl, 400 mM sucrose (Ultragrade, BDH), and 100 μM EGTA. The Ca^{2+}-depleted PSII membranes were collected by centrifugation for 20 min at 36000*g* and 4 °C and resuspended in a similar buffer medium containing 25 mM MES/NaOH (pH 6.3), 15 mM NaCl, 400 mM sucrose (Ultragrade, BDH), and either 50 mM $SrCl_2$, 50 mM $CaCl_2$, or no other additions. The samples suspended in the $SrCl_2$- or $CaCl_2$-containing buffers were allowed to incubate for 2−3 h at 4 °C. Finally, the samples were pelleted and resuspended in a small amount of the supernatant before being snap-frozen in liquid N_2 and stored at −80 °C until the measurements could be taken.

Alternatively, the functional Ca^{2+} was depleted from the OEC using a NaCl/A23187/EGTA treatment, which also removes the 17 and 23 kDa extrinsic proteins (*9*, *18*). Samples treated in this manner are called "Ca^{2+}/Ex-depleted". In this case, PSII-enriched membranes were suspended to a density of 0.5 mg of Chl/mL in 40 mM MES/NaOH (pH 5.0), 1.5 M NaCl, 1 mM EGTA, and the Ca^{2+} ionophore A23187 (20 μM), and the mixture was gently stirred for 2.5 h in the dark at 4 °C. The sample was pelleted by centrifugation for 20 min at 36000*g* and 4 °C and washed using the same buffer medium but without A23187. The sample was then resuspended in a second buffer medium consisting of 40 mM MES/NaOH (pH 6.3), 400 mM sucrose (Ultragrade, BDH), 15 mM NaCl, and 1 mM EGTA. The sample was then washed two more times in the same buffer medium but without EGTA. The Ca^{2+}/Ex-depleted PSII membranes were resuspended in the same wash buffer (without EGTA) containing either 50 mM $SrCl_2$, 50 mM

$CaCl_2$, or no other additions. The samples suspended in the $SrCl_2$- or $CaCl_2$-containing buffers were allowed to incubate for 2−3 h at 4 °C. Finally, the samples were pelleted and resuspended in a small amount of the supernatant before being snap-frozen in liquid N_2 and stored at −80 °C until the measurements could be taken. All glassware and centrifuge tubes used in the Ca^{2+} depletion procedures were washed with 2 M HNO_3, and the buffers were treated with Chelex-100 (Bio-Rad) to ensure minimal Ca^{2+} contamination from the reagents that were used.

O_2 Evolution Measurements. Initial steady-state rates of O_2 evolution were measured at 25 °C using a Clark-type electrode (Hansatech) under continuous saturating illumination (custom-built 150 W tungsten light source, viz. >5000 μmol m^{-2} s^{-1}). A typical assay contained 10 μg of Chl/mL with 1 mM $K_3Fe(CN)_6$ and 400 μM phenyl-*p*-benzoquinone (PPBQ) as electron acceptors in the final suspension medium for each particular sample. Chlorophyll concentrations were determined according to the method of Porra et al. (*52*).

Mass Spectrometric Measurements. Isotopic determinations of the flash-induced O_2 produced by PSII-enriched samples were made at *m*/*e* 34 and 36 using an in-line mass spectrometer (Vacuum Generation MM6, Winsford) as described previously (*53*, *54*). A stirred, closed chamber system was used for the rapid equilibration of 25 μL of $H_2{}^{18}O$ (98.5% enrichment, Isotech, Miamisberg, OH) into 160 μL of the sample. Injection of the labeled water was achieved using a Hamilton CR700-200 spring-loaded syringe triggered by a computer-actuated solenoid. Samples were activated using saturating light flashes (fwhh ∼ 8 μs) provided by a battery of xenon flash lamps (FX-1163 lamp with internal reflector, 4 μF at 1 kV capacitor, EG&G, Salem, MA) through a fiber optic situated directly in front of the sample chamber window. The flash/injection protocols used to assess the ^{18}O exchange in the various S states are given in Figure 1 of ref *55* and were controlled via a computer. Accurate timing intervals were established from a digital oscilloscope (Tektronix, model 350).

The ^{18}O exchange measurements were taken in the presence of 1 mM $K_3Fe(CN)_6$ and 400 μM PPBQ. Samples were first preset in the S_1 state by a preflash followed by a 10 min dark period at room temperature. For each exchange measurement, electron acceptors were added to an aliquot, and the aliquot was loaded into the sample chamber in the dark and degassed for 10 min at 10 °C prior to the particular flash/injection sequence. For an optimal signal-to-noise (S/N) ratio, the sample concentration was adjusted to 0.5 mg of Chl/mL for the S_3-state measurement and to 0.2 mg of Chl/mL for the S_2- and S_1-state measurements using the final suspension medium for each particular sample. After the rapid turnover flashes were given, due to the time it takes for the gas to diffuse from the sample chamber to the ionizing source of the mass spectrometer, a series of normalization flashes were applied at 0.05 Hz. To minimize S-state deactivation between the normalization flashes, measurements were taken at 10 °C.

The O_2 background introduced into the sample during the injection of $H_2{}^{18}O$ was subtracted from the photogenerated O_2 by performing a pre-injection under the same conditions but without illumination. To reduce the size of the O_2 background, small quantities of glucose, glucose oxidase, and catalase were added to the labeled water prior to injection without interference from the photogenerated O_2. The signal amplitude for the third flash (Y_3) in the turnover sequence, less the contribution from the injection (Y_{inj}) and double hits (Y_{2x}, as calculated in ref *56*), was normalized to the sum of flashes 4−7 given in the normalization sequence, to correct for small variations in sample concentration and membrane permeability between different measurements

$$Y_{3N} = \frac{(Y_3 - Y_{inj} - Y_{2x})}{\sum_{n=4}^{7} Y_n} \quad (1)$$

The Y_{3N} value at each exchange time was then further normalized to the value obtained after complete exchange (i.e., 10 s) to give Y_{3C}. Finally, the data at fast exchange times (≤10 ms) was corrected for the 175 s^{-1} injection response of the sample chamber as described in ref *54*. The level of ^{18}O enrichment (ϵ) in the sample chamber was ∼12%, as determined according to ref *56*.

At *m*/*e* 34, plots of the corrected O_2 yields after the third flash, $^{34}Y_{3C}$, versus the ^{18}O exchange time in a particular S state, Δt, are clearly biphasic and were analyzed as the sum of two exponentials:

$$^{34}Y_{3C} = 0.57[1 - \exp(-{}^{34}k_2 t)] + 0.43[1 - \exp(-{}^{34}k_1 t)] \quad (2)$$

where the relative contributions from the two phases follow from the isotopic distribution due to exchange at two independent sites (*54*).

In contrast, at *m*/*e* 36, plots of $^{36}Y_{3C}$ versus Δt exhibit only one kinetic phase and were analyzed in terms of a single exponential:

$$^{36}Y_{3C} = [1 - \exp(-{}^{36}kt)] \quad (3)$$

Sigma Plot (SPSS, Chicago, IL) was used to fit the data according to eqs 2 and 3.

RESULTS

Extraction procedures for removal of the functional Ca^{2+} from the OEC typically employ a combination of NaCl, chelator(s) (e.g., Chelex 100 and/or citrate, EGTA, and EDTA), illumination, low pH, and the Ca^{2+} specific ionophore A23187 (*9*, *18*, *51*). The exposure to a high ionic strength using high concentrations of NaCl (i.e., >1 M) in some treatments (*9*, *18*) targets the specific removal of the 17 and 23 kDa extrinsic proteins, which are known to enhance the binding affinity of Ca^{2+} (*18*, *19*). In contrast, the low-pH/citrate treatment induces a temporary dislocation of these proteins, which rebind to PSII upon restoring a neutral pH (*57*). In this study, we used both a low-pH/citrate treatment and an NaCl/A23187/EGTA treatment to remove the functional Ca^{2+} from the OEC. In the former case, we found in our samples that ∼80% of the 33, 23, and 17 kDa extrinsic proteins are retained after treatment. In the latter case, ∼90% of the 33 kDa extrinsic protein and only ∼2% of the 23 and 17 kDa extrinsic proteins are retained after treatment (*58*).

Upon removal of the functional Ca^{2+} from the OEC, the steady-state rate of O_2 evolution is largely inhibited. This is shown in Table 1 where the residual activity of Ca^{2+}-depleted

Table 1: O_2-Evolving Activities and Kok Parameters for PSII Samples Depleted of Ca^{2+} and Reconstituted with Ca^{2+} or Sr^{2+}

	O_2 evolution			
	activity[a]	% control	α[b]	β[c]
untreated PSII	681 ± 9	100	0.119	0.046
Ca^{2+}-depleted PSII[d]	34 ± 7	5	nd[e]	nd[e]
Ca^{2+}-depleted PSII with $CaCl_2$[f]	429 ± 19	63	0.175	0.065
Ca^{2+}-depleted PSII with $SrCl_2$[g]	219 ± 32	32	0.192	0.081
untreated PSII	767 ± 11	100	0.101	0.042
Ca^{2+}/Ex-depleted PSII[h]	15 ± 8	2	nd[e]	nd[e]
Ca^{2+}/Ex-depleted PSII with $CaCl_2$[i]	360 ± 15	47	0.181	0.073
Ca^{2+}/Ex-depleted PSII with $SrCl_2$[j]	146 ± 22	19	0.217	0.092

[a] Rates of O_2 evolution expressed as micromoles of O_2 per milligram of Chl per hour. [b] Fraction of misses. [c] Fraction of double hits. [d] PSII membranes subjected to low-pH/citrate treatment and depleted of Ca^{2+}. [e] Not determined. [f] PSII membranes subjected to low-pH/citrate treatment and reconstituted with Ca^{2+}. [g] PSII membranes subjected to low-pH/citrate treatment and reconstituted with Sr^{2+}. [h] PSII membranes subjected to NaCl/A23187/EGTA treatment and depleted of Ca^{2+} and the 17 and 23 kDa extrinsic proteins. [i] PSII membranes subjected to NaCl/A23187/EGTA treatment and reconstituted with Ca^{2+}. [j] PSII membranes subjected to NaCl/A23187/EGTA treatment and reconstituted with Sr^{2+}. See the text for details.

and Ca^{2+}/Ex-depleted samples is only 2−5% of the untreated control. Significant restoration of activity is achieved by incubating the depleted samples in either 50 mM $CaCl_2$ or 50 mM $SrCl_2$ for extended periods of time (viz. 2−3 h). The rates of O_2 evolution for the Ca^{2+}-depleted samples recover to ~63% of the untreated control upon incubation with $CaCl_2$ and to ~32% upon incubation with $SrCl_2$, while for the Ca^{2+}/Ex-depleted samples, the recovered activities are ~47 and ~19%, respectively.

Figure 1 shows the normalized O_2 flash yield patterns at *m*/*e* 34 for Ca^{2+}-depleted and Ca^{2+}/Ex-depleted samples reconstituted with Ca^{2+} or Sr^{2+}. The measurements were taken at 10 °C following complete isotopic equilibration after the addition of $H_2{}^{18}O$ (i.e., at an exchange time of >10 s). The depleted samples reveal normal period 4 oscillations in the presence of either $CaCl_2$ or $SrCl_2$. The respective miss (α) and double hit (β) parameters as determined by the Kok method of analysis (*1*, *2*) are listed in Table 1. The relatively heavier damping in O_2 flash yield oscillations for the reconstituted samples correlates with the overall reduced steady-state O_2-evolving activities; however, the period 4 oscillations indicate that normal turnover of the S-states occurs.

To determine the effect(s) of Sr^{2+} replacement at the Ca^{2+} site on the behavior of substrate-water binding, the rates of ^{18}O exchange were determined for Ca^{2+}-depleted and Ca^{2+}/Ex-depleted samples reconstituted with Sr^{2+}. Depleted samples reconstituted with Ca^{2+} are considered to be the controls in these measurements. Isotopic determinations of the flash-induced O_2 produced by the Ca^{2+}- and Sr^{2+}-reconstituted samples were recorded at *m*/*e* 34 in the S_1 and/or the S_2 and S_3 states at 10 °C. The results are shown in Figure 2 for Ca^{2+}-depleted samples and in Figure 3 for Ca^{2+}/Ex-depleted samples. In these measurements, the corrected O_2 yields after the third flash in the turnover sequence ($^{34}Y_{3C}$) are plotted as a function of the $H_2{}^{18}O$ exchange time (Δt) in the various S states. In both Ca^{2+}-depleted and Ca^{2+}/Ex-depleted samples, upon reconstitution with either Ca^{2+} or Sr^{2+}, the exchange data exhibit strong biphasic behavior in

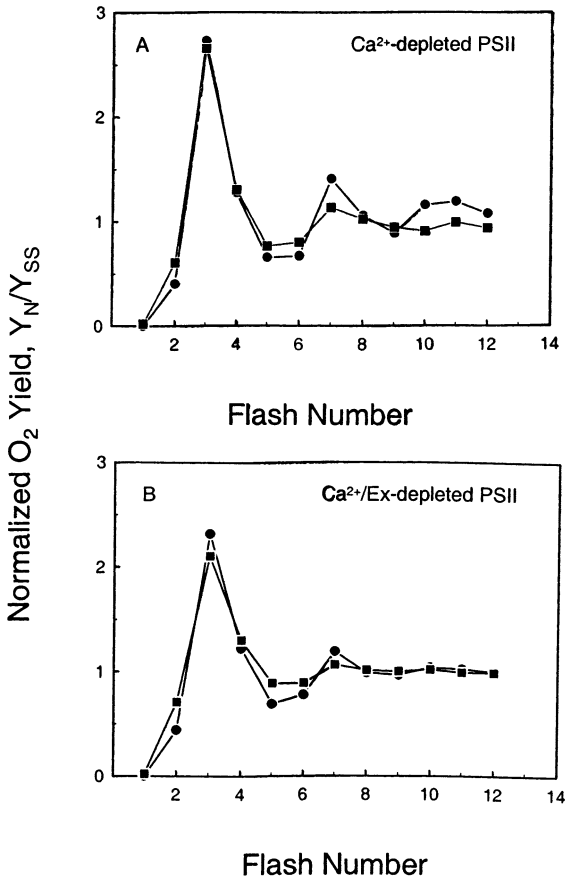

FIGURE 1: O_2 flash yields normalized to the same steady-state value for (A) Ca^{2+}-depleted PSII samples prepared by low-pH/citrate treatment and (B) Ca^{2+}/Ex-depleted PSII samples prepared by NaCl/A23187/EGTA treatment and reconstituted with Ca^{2+} (●) or Sr^{2+} (■). Measurements were taken at *m*/*e* 34 following complete isotopic equilibration upon addition of $H_2{}^{18}O$ at 10 °C. The derived miss and double hit parameters according to the Kok model are listed in Table 1.

all of the S states that were assessed. As calculated according to eq 2, the corresponding rate constants for the slowly and quickly exchanging components are listed in Table 2. Comparisons of these data indicate that the overall rates of slow ^{18}O exchange for Ca^{2+}-reconstituted samples in the S_3, S_2, and S_1 states are very similar to those for intact PSII-enriched membrane samples, as taken from ref *59*. In the S_3 state, the fast ^{18}O exchange is also virtually unaffected; however, as in the control, the rates of fast exchange in the S_2 and S_1 states are unresolved, where $^{34}k_2 > 175\ s^{-1}$ and $^{34}k_2 > 100\ s^{-1}$, respectively.

The most significant finding is revealed by the data for the slow ^{18}O exchange in Sr^{2+}-reconstituted samples (Figures 2 and 3 and Table 2). In the S_3 state for the Ca^{2+}-depleted samples, there is an ~3−4-fold increase in the slow exchange rate ($^{34}k_1$) from 1.4 ± 0.1 s^{-1} in the Ca^{2+}-reconstituted control to 5.2 ± 1.6 s^{-1} in the Sr^{2+}-reconstituted sample. Interestingly, the same trend is observed in the earlier S states as well, where the slow exchange rates ($^{34}k_1$) increase from 2.1 ± 0.3 to 7.7 ± 2.4 s^{-1} in the S_2 state and from 0.023 ± 0.002 s^{-1} to 0.082 ± 0.012 s^{-1} in the S_1 state. Similarly, for the Ca^{2+}/Ex-depleted samples, the slow ^{18}O exchange rates ($^{34}k_1$) also increase upon Sr^{2+} reconstitution, from 1.5 ± 0.2 to 5.1 ± 2.1 s^{-1} in the S_3 state and from 1.5 ± 0.5 to 5.3 ± 1.4 s^{-1} in the S_2 state. In contrast, the fast ^{18}O exchange

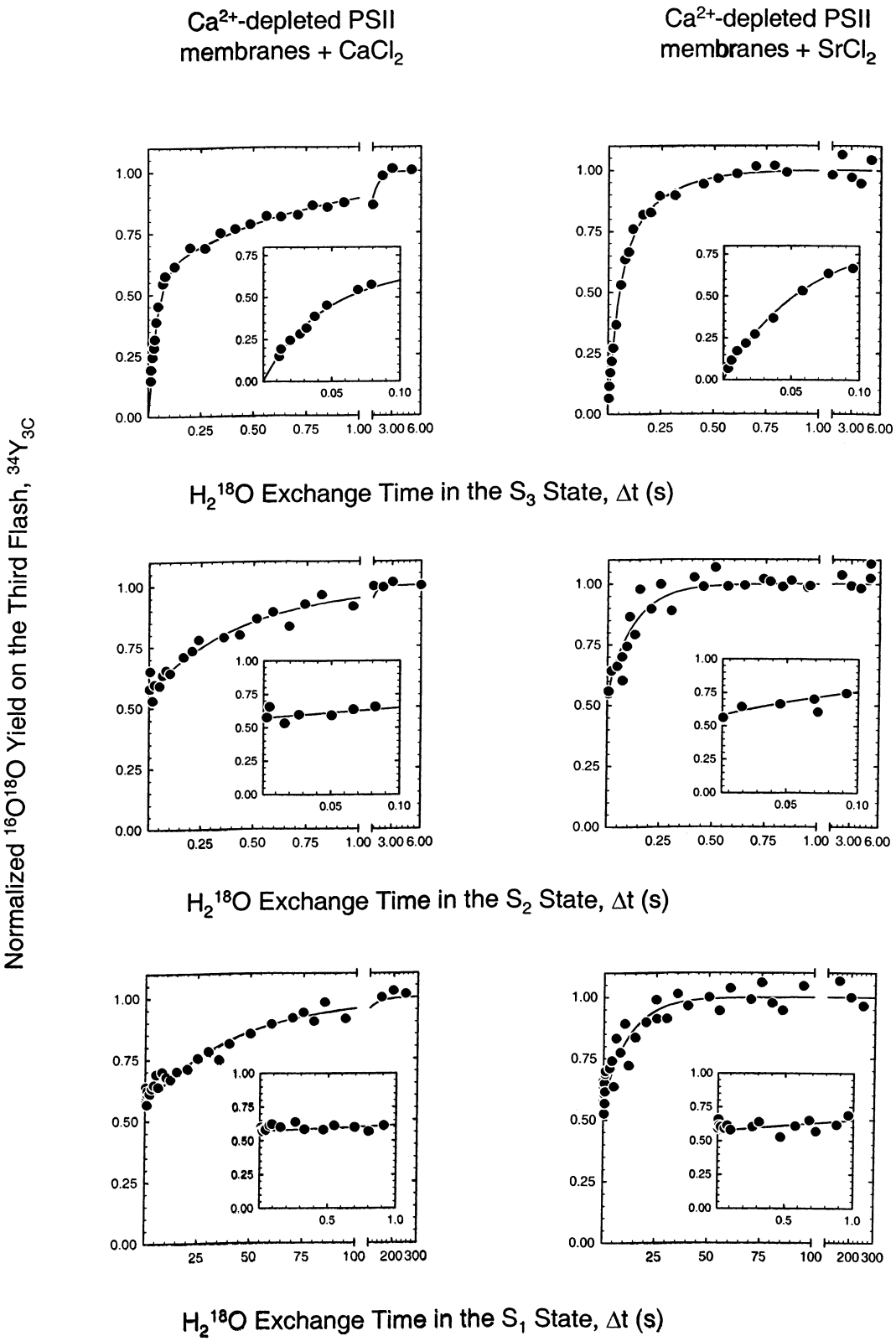

FIGURE 2: ^{18}O exchange measurements in the S_3, S_2, and S_1 states taken at *m*/*e* 34 for Ca^{2+}-depleted PSII samples prepared by low-pH/citrate treatment and reconstituted with Ca^{2+} or Sr^{2+}. Measurements were taken as a function of the exchange time (Δt) in each S state at 10 °C. Solid lines are kinetic fits to the data according to eq 2. The insets reveal expanded time ordinates for the first 100 ms in the S_3 and S_2 states and for first 1000 ms in the S_1 state.

when measured in the S_3 state in either the Ca^{2+}-depleted or the Ca^{2+}/Ex-depleted sample is not significantly influenced by Sr^{2+} reconstitution. These results clearly indicate that the two types of Ca^{2+} depletion procedures are affecting the same site.

To confirm these observations, measurements were also taken at *m*/*e* 36 for Sr^{2+}-reconstituted, Ca^{2+}-depleted preparations in the S_3 and S_2 states, which provides an independent measure of $^{34}k_1$. The data are presented in Figure 4 and, as expected, reveal monoexponential kinetics. The correspond-

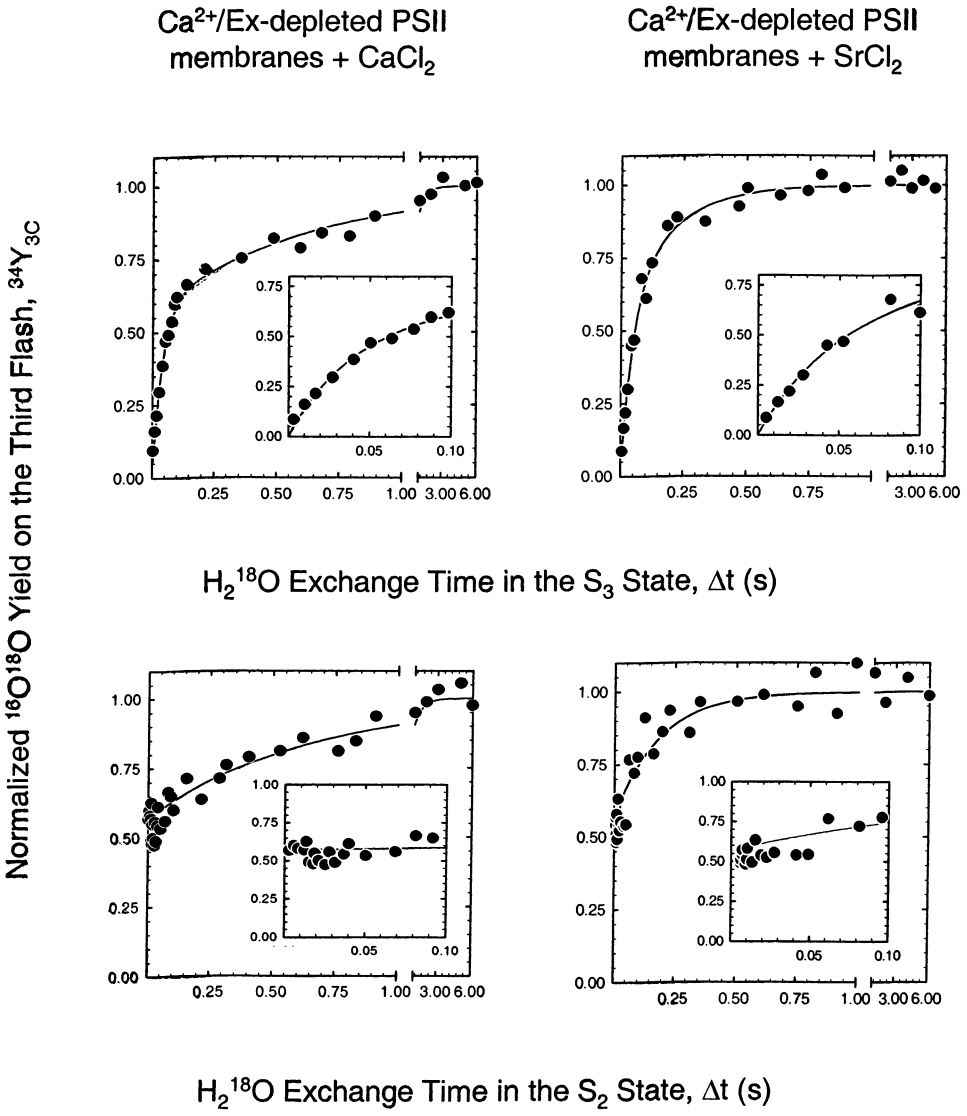

FIGURE 3: ^{18}O exchange measurements in the S_3 and S_2 states taken at *m/e* 34 for Ca^{2+}/Ex-depleted PSII samples prepared by NaCl/A23187/EGTA treatment and reconstituted with Ca^{2+} or Sr^{2+}. The measurements were taken as a function of the exchange time (Δt) in each S state at 10 °C. Solid lines are kinetic fits to the data according to eq 2. The insets reveal expanded time ordinates for the first 100 ms in the S_3 and S_2 states.

Table 2: ^{18}O Exchange Rate Constants Determined at *m/e* 34 and 36 for Ca^{2+}- and Sr^{2+}-Reconstituted Photosystem II Samples

	^{18}O exchange rate constants at 10 °C								
	S_3 state			S_2 state			S_1 state		
	$^{34}k_1$ (s^{-1})	$^{34}k_2$ (s^{-1})	^{36}k (s^{-1})	$^{34}k_1$ (s^{-1})	$^{34}k_2$ (s^{-1})	^{36}k (s^{-1})	$^{34}k_1$ (s^{-1})	$^{34}k_2$ (s^{-1})	^{36}k (s^{-1})
untreated PSII[a]	2.5 ± 0.2	30 ± 2	2.4 ± 0.2	1.9 ± 0.3	≥ 175	2.1 ± 0.3	0.022 ± 0.003	>100	nd[b]
Ca^{2+}-depleted PSII with $CaCl_2$[c]	1.4 ± 0.1	27 ± 2	nd[b]	2.1 ± 0.3	≥ 175	nd[b]	0.023 ± 0.002	>100	nd[b]
Ca^{2+}/Ex-depleted PSII with $CaCl_2$[d]	1.5 ± 0.2	27 ± 3	nd[b]	1.5 ± 0.5	>175	nd[b]	nd[b]	nd[b]	nd[b]
Ca^{2+}-depleted PSII with $SrCl_2$[e]	5.2 ± 1.6	23 ± 5	5.8 ± 0.3	7.7 ± 2.4	≥ 175	9.4 ± 0.6	0.082 ± 0.012	>100	nd[b]
Ca^{2+}/Ex-depleted PSII with $SrCl_2$[f]	5.1 ± 2.1	22 ± 6	nd[b]	5.3 ± 1.4	>175	nd[b]	nd[b]	nd[b]	nd[b]

[a] Exchange rate constants obtained from ref *59*. [b] Not determined. [c] PSII membranes subjected to low-pH/citrate treatment and reconstituted with Ca^{2+}. [d] PSII membranes subjected to NaCl/A23187/EGTA treatment and reconstituted with Ca^{2+}. [e] PSII membranes subjected to low-pH/citrate treatment and reconstituted with Sr^{2+}. [f] PSII membranes subjected to NaCl/A23187/EGTA treatment and reconstituted with Sr^{2+}. See the text for details.

ing rate constants given in Table 2 are as follows: $^{36}k = 5.8 \pm 0.3$ s^{-1} for the S_3 state, and $^{36}k = 9.4 \pm 0.6$ s^{-1} for the S_2 state. These values compare reasonably well with the rates obtained for the slow exchange in the *m/e* 34 data upon Sr^{2+} reconstitution in both the Ca^{2+}-depleted and Ca^{2+}/Ex-depleted samples (Table 2). These data clearly indicate a Sr^{2+} specific effect on the rate of the slow ^{18}O exchange across each of the S states that were assessed.

DISCUSSION

Although the exact role of Ca^{2+} in O_2 evolution remains unresolved, numerous experimental data demonstrate a

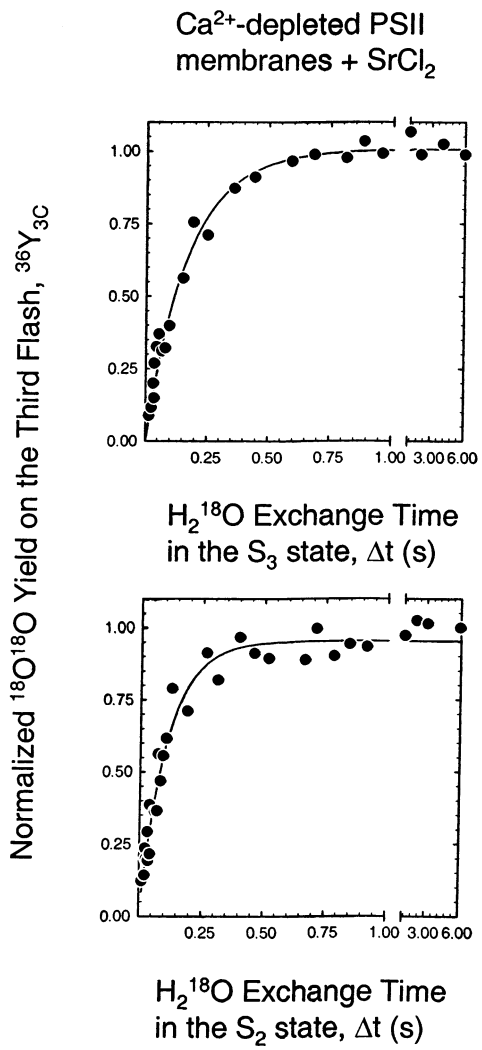

FIGURE 4: ^{18}O exchange measurements in the S_3 and S_2 states taken at *m*/*e* 36 for Ca^{2+}-depleted PSII samples prepared by low-pH/citrate treatment and reconstituted with Sr^{2+}. The measurements were taken as a function of the exchange time (Δt) in each S state at 10 °C. Solid lines are kinetic fits to the data according to eq 3.

structural and functional intimacy of Ca^{2+} with the OEC. Recent proposals suggest that Ca^{2+} plays a direct role in the water oxidation chemistry, in particular, by acting as a substrate-binding site which orients a water molecule in a nucleophilic attack during the $S_3 \rightarrow [S_4] \rightarrow S_0$ transition (*45*−*48*). In an effort to address these proposals, the rates of ^{18}O exchange were determined for PSII-enriched membrane preparations depleted of Ca^{2+} and subsequently reconstituted with either Sr^{2+} or Ca^{2+}.

Because of the selectivity of the mass spectrometric measurements (i.e., detection of centers that are only active in O_2 evolution), determination of the rate of ^{18}O exchange in Ca^{2+}- and Sr^{2+}-reconstituted PSII samples provides a useful probe for the involvement of Ca^{2+} in substrate-water binding. Since Sr^{2+} is the only other metal ion that replaces Ca^{2+} and still maintains O_2-evolving activity (*18*), the application of this technique cannot be extended to studies in which the Ca^{2+} site is occupied by other metal ions with similar (or dissimilar) physical properties (e.g., Cd^{2+}, La^{3+}, or Dy^{3+}).

We reported earlier that small variations in the rate constants for the two phases of ^{18}O exchange can occur depending on the source and type of sample preparation (*60*). For example, the rate of slow exchange in the S_3 state in spinach thylakoids is approximately twice the rate of slow exchange in spinach core particles and half the rate of slow exchange in *Synechocystis* thylakoids. However, the fact that the ^{18}O exchange in Ca^{2+}-reconstituted samples is not terribly different from the ^{18}O exchange in native PSII (Table 2) indicates that the structural and functional integrity of the OEC is not dramatically perturbed by the extraction or reconstitution procedures used in this study. Hence, changes in the exchange behavior upon reconstitution with Sr^{2+} can be ascribed directly to the effects of occupation of the Ca^{2+} site by Sr^{2+}.

Comparison of the rates of slow ^{18}O exchange (i.e., $^{34}k_1$) upon Sr^{2+} reconstitution in both Ca^{2+}-depleted and Ca^{2+}/Ex-depleted samples clearly shows an ∼3−4-fold increase with respect to the slow exchange upon Ca^{2+} reconstitution (Figures 2 and 3 and Table 2). Most importantly, the relative magnitude of this increase is maintained throughout all of the S states that have been assessed (i.e., S_3, S_2, and S_1) (Figures 2 and 3 and Table 2). As an independent measure of the slow exchange, the single-exponential kinetics from the *m*/*e* 36 data for Sr^{2+}-reconstituted, Ca^{2+}-depleted samples were also determined, since the doubly labeled $^{18}O_2$ product is limited by the slowest ^{18}O exchange process (*54*). In these measurements as well, the rate of ^{18}O exchange upon Sr^{2+} reconstitution was found to be increased, where the ^{36}k values are comparable to the $^{34}k_1$ values in the S_3 and S_2 states (Figures 2 and 4 and Table 2). Thus, there is a distinct Sr^{2+} specific effect on the slow ^{18}O exchange.

On the other hand, the rate for the fast ^{18}O exchange remains relatively unaffected upon Sr^{2+} reconstitution, in either Ca^{2+}-depleted or Ca^{2+}/Ex-depleted samples in the S_3 state (Figure 2 and Table 2). In the latter case, we may have expected a small decrease in the rate of fast exchange, since we observed earlier that the removal of the 17 and 23 kDa extrinsic proteins by a simple salt wash leads to an ∼30% decrease in the rate of fast exchange, with or without the addition of $CaCl_2$ (*59*). However, there was no obvious decrease, within the experimental error of the measurements, so we must assume that other aspects of the extraction procedures obscure this effect. As a consequence, the fast exchange in the S_2 (or the S_1) state could not be resolved in these samples. Regardless, it is clear that the slow ^{18}O exchange is affected by Sr^{2+} reconstitution while the detectable fast exchange is not, in contrast to earlier expectations (*47*, *53*).

The Sr^{2+} ion has an inherently larger ionic radius than the Ca^{2+} ion (1.12 and 0.99 Å, respectively). A larger ionic radius results in lengthened bonds, reduced hydration enthalpy, and a tendency toward increased coordination geometry (*61*−*64*). Thus, it can be expected that the corresponding ligand exchange for Sr^{2+} will be faster than for Ca^{2+}. Using the normal Eyring relation between the rate constant and the activation free energy [$\log(k/k') \sim \Delta(\Delta G) \sim \Delta pK$] and the difference in proton binding affinities between Sr^{2+} and Ca^{2+} ions in water ($\Delta pK \sim 0.4$) (*64*), the water exchange rate for the aqua complex of Sr^{2+} is estimated to be ∼3 times faster than for Ca^{2+}. Since the slow ^{18}O exchange in all of the S states that were assessed is accelerated ∼3−5-fold upon Sr^{2+} reconstitution compared with Ca^{2+} reconstitution, it is attractive to suggest that the

slowly exchanging component directly involves a Ca^{2+} (Sr^{2+}) interaction.

The rates of water exchange for hydrated metal ion complexes have been extensively characterized (reviewed in refs *61*−*63*). For $[Ca(OH_2)_{6-10}]^{2+}$ and $[Sr(OH_2)_6]^{2+}$ complexes, the rates of water exchange are on the order of 10^8-10^9 s^{-1}, which is 7−8 orders of magnitude larger than the rates of slow exchange in Ca^{2+}- and Sr^{2+}-reconstituted PSII (where $^{34}k_1$ is in the range of 10^0-10^1 s^{-1}). If substrate water is indeed bound to Ca^{2+}, then it is important to consider factors that can slow the exchange kinetics. The most likely of these to be relevant for PS II are the positive charge density of the Mn_4 cluster and the steric hindrance by the immediate (and distal) ligand environment. As discussed above, we showed that the removal of the 17 and 23 kDa extrinsic proteins, which represents an accessibility barrier to the Mn_4 cluster by exogenous reductants (*65*), has no effect on the slow exchange and at most only a small effect (∼30% decrease) on the fast exchange (*59*). Thus, the effect of steric hindrance is likely to be small by comparison. On the other hand, the positive charge density on the Mn_4 cluster may have a quite strong influence.

On the basis of the XANES assignment of Mn oxidation states, it is generally accepted that the Mn_4 cluster is predominantly composed of Mn(III) and Mn(IV) ions [see the special issue on photosynthetic water oxidation of *Biochimica et Biophysica Acta* (2001) *1503*, 1−259]. However, the water exchange rates for hydrated Mn(III) and Mn(IV) ions are not known, as the strong oxidizing potential of these ions dictates that they do not readily exist as aqueous ions in solution. Nevertheless, a comparative analysis with Fe or Ru ions in different oxidation states reveals that the water exchange rate in general decreases by $\sim10^4$ for a formal oxidation state increase from +2 to +3 (*61*). Similarly, a comparison with the Cr(III) ion provides an estimate for the water exchange rate at Mn(IV) since the two ions are isoelectronic. It therefore can be expected that the water exchange rates for hydrated Mn(IV) should be in the range of $10^{-6}-10^{-4}$ s^{-1}, while for hydrated Mn(III), they should be in the range of $10^{-2}-10^{0}$ s^{-1} (*61*). These predictions are in close agreement with the computational analysis by Kuzek and Pace (*48*), where the water ligand exchange rates in the primary coordination sphere of $Mn(III)(H_2O)_6$ and $Mn(IV)(H_2O)_6$ were estimated to be in the range of 10^0-10^1 and $10^{-7}-10^{-8}$ s^{-1}, respectively. Thus, if Ca^{2+} is indeed involved in the binding of substrate water, it may be possible to reconcile the overall magnitude of the observed slow exchange rate (i.e., $^{34}k_1 = 10^0-10^1$ s^{-1}) by invoking a bridging structure between Ca^{2+} and a higher-oxidation state Mn ion. In this hypothesis, the isotopic exchange of the bound substrate would be modulated by the influence of two very different ionic configurations. The isotopic exchange at such a site can be simply depicted as

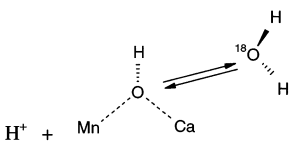

However, it is important to keep in mind that factors other than the oxidation state and ionic radii can also have a major impact on the substrate-water exchange. Of particular relevance would be H-bonding networks, which have been shown to be important for proton-coupled electron transfers in PSII [see the special issue on photosynthetic water oxidation of *Biochimica et Biophysica Acta* (2001) *1503*, 1−259]. It has been suggested that a Ca^{2+}-bound water forms a H-bond with the bridging oxygen in a $Mn_2(\mu\text{-}O)_2$ unit (*47*, *66*). Thus, upon substitution of the Ca^{2+} site with Sr^{2+}, the local H-bonding network may be altered such that the exchange rate of the slowly exchanging water increases at a nearby though chemically different site. Evaluation of H-bonding contributions, however, will require further advances in our knowledge of the molecular structure of PSII. Similarly, the influence of the functional Ca^{2+} on the binding of the substrate water could also be exerted through secondary, outer sphere effects, for example, by controlling the approach of the solvent to the slowly exchanging site (*23*). To determine this as well will require further studies on the molecular structure of PSII. Although it is not possible to discern the precise chemical nature of the substrate binding sites at this time, the results reported in this study do clearly reveal an inherent interaction between the binding of one of the substrate-water molecules and the functional Ca^{2+}.

ACKNOWLEDGMENT

We sincerely thank Drs. Warwick Hillier and Charles Dismukes for many fruitful discussions of this work and offering many useful suggestions. We also thank Mr. Joel Freeman for assistance in the preparation of the manuscript.

REFERENCES

1. Kok, B., Forbush, B., and McGloin, M. (1970) *Photochem. Photobiol. 11*, 457−475.
2. Forbush, B., Kok, B., and McGloin, M. (1971) *Photochem. Photobiol. 14*, 307−321.
3. Yocum, C. F. (1991) *Biochim. Biophys. Acta 1059*, 1−15.
4. Debus, R. J. (1992) *Biochim. Biophys. Acta 1102*, 269−352.
5. Han, K.-C., and Katoh, S. (1993) *Plant Cell Physiol. 34*, 585−593.
6. Han, K.-C., and Katoh, S. (1995) *Biochim. Biophys. Acta 1232*, 230−236.
7. Chen, C., and Cheniae, G. M. (1995) in *Photosynthesis: from Light to the Biosphere* (Mathis, P., Ed.) pp 329−332, Kluwer Academic Publishers, Dordrecht, The Netherlands.
8. Ädelroth, P., Lindberg, K., and Andreasson, L.-E. (1995) *Biochemistry 34*, 9201−9207.
9. Kalosaka, K., Beck, W. F., Brudvig, G., and Cheniae, G. (1990) *Curr. Res. Photosynth. 1*, 721−724.
10. Grove, G. N., and Brudvig, G. W. (1998) *Biochemistry 37*, 1532−1539.
11. Ghanotakis, D. F., Topper, J. N., Babcock, G. T., and Yocum, C. F. (1984) *FEBS Lett. 170*, 169−173.
12. Ono, T., and Inoue, Y. (1989) *Arch. Biochem. Biophys. 275*, 440−448.
13. Boussac, A., and Rutherford, A. W. (1988) *FEBS Lett. 236*, 432−436.
14. Boussac, A., Sétif, P., and Rutherford, A. W. (1992) *Biochemistry 31*, 1224−1234.
15. Westphal, K. L., Lydakis-Simantris, N., Cukier, R. I., and Babcock, G. T. (2000) *Biochemistry 39*, 16220−16229.
16. Ghanotakis, D. F., Babcock, G. T., and Yocum, C. F. (1985) *FEBS Lett. 192*, 1−3.
17. Miyao, M., and Murata, N. (1984) *FEBS Lett. 168*, 118−120.
18. Vrettos, J. S., Stone, D. A., and Brudvig, G. W. (2001) *Biochemistry 40*, 7937−7945.
19. Vander Meulen, K. A., Hobson, A., and Yocum, C. F. (2002) *Biochemistry 41*, 958−966.
20. Ono, T.-A., Rompel, A., Mino, H., and Chiba, N. (2001) *Biophys. J. 81*, 1831−1840.

21. Kimura, Y., Hasegawa, K., and Ono, T.-A. (2002) *Biochemistry 41*, 5844−5853.
22. Boussac, A., Zimmerman, J.-L., and Rutherford, A. W. (1989) *Biochemistry 28*, 8984−8989.
23. Sivaraja, M., Tso, J., and Dismukes, G. C. (1989) *Biochemistry 28*, 9459−9464.
24. Ono, T., and Inoue, Y. (1990) *Biochim. Biophys. Acta 1020*, 269−277.
25. Boussac, A., Zimmerman, J.-L., and Rutherford, A. W. (1990) *FEBS Lett. 277*, 69−74.
26. Boussac, A., Zimmerman, J.-L., Rutherford, A. W., and Lavergne, J. (1990) *Nature 347*, 303−306.
27. Berthomieu, C., and Boussac, A. (1995) *Biochemistry 34*, 1541−1548.
28. Hallahan, B. J., Nugent, J. H. A., Warden, J. T., and Evans, M. C. W. (1992) *Biochemistry 31*, 4562−4573.
29. Gilchrist, M. L., Ball, J. A., Randall, D. W., and Britt, R. D. (1995) *Proc. Natl. Acad. Sci. U.S.A. 92*, 9545−9549.
30. Tang, X. S., Randall, D. W., Force, D. A., Diner, B. A., and Britt, R. D. (1996) *J. Am. Chem. Soc. 118*, 7638−7639.
31. Force, D. A., Randall, D. W., and Britt, R. D. (1997) *Biochemistry 36*, 12062−12070.
32. Zouni, A., Witt, H. T., Kern, J., Fromme, P., Krauss, N., Saenger, W., and Orth, P. (2001) *Nature 409*, 739−743.
33. Kamiya, N., and Shen, J.-R. (2003) *Proc. Natl. Acad. Sci. U.S.A. 100*, 98−103.
34. Booth, P. J., Rutherford, A. W., and Boussac, A. (1996) *Biochim. Biophys. Acta 1277*, 127−134.
35. Matysik, J., Nachtegaal, G., van Gorkom, H. F., Hoff, A. J., and de Groot, H. J. M. (2000) *Biochemistry 39*, 6751−6755.
36. Latimer, M. J., DeRose, V. J., Mukerji, I., Yachandra, V. K., Sauer, K., and Klein, M. P. (1995) *Biochemistry 34*, 10898−10909.
37. Cinco, R. M., Robblee, J. H., Rompel, A., Fernandez, C., Yachandra, V. K., Sauer, K., and Klein, M. P. (1998) *J. Phys. Chem. B 102*, 8248−8256.
38. Latimer, M. J., DeRose, V. J., Yachandra, V. K., Sauer, K., and Klein, M. P. (1998) *J. Phys. Chem. B 102*, 8257−8265.
39. Robblee, J. H., Cinco, R. M., and Yachandra, V. K. (2001) *Biochim. Biophys. Acta 1503*, 7−23.
40. Yachandra, V. K., DeRose, V. J., Latimer, M. J., Mukerji, I., Sauer, K., and Klein, M. P. (1993) *Science 260*, 675−679.
41. Noguchi, T., Ono, T.-A., and Inoue, Y. (1995) *Biochim. Biophys. Acta 1228*, 189−200.
42. Ghanotakis, D. F., and Yocum, C. F. (1990) *Annu. Rev. Plant Physiol. Mol. Plant Biol. 41*, 255−276.
43. Rutherford, A. W. (1989) *Trends Biochem. Sci. 14*, 227−232.
44. Tommos, C., and Babcock, G. T. (1998) *Acc. Chem. Res. 31*, 18−25.
45. Pecoraro, V. L., Baldwin, M. J., Caudle, M. T., Hsieh, W.-Y., and Law, N. A. (1998) *Pure Appl. Chem. 70*, 925−929.
46. Siegbahn, P. E. (2000) *Inorg. Chem. 39*, 2923−2935.
47. Vrettos, J. S., Limburg, J., and Brudvig, G. W. (2001) *Biochim. Biophys. Acta 1503*, 229−245.
48. Kuzek, D., and Pace, R. J. (2001) *Biochim. Biophys. Acta 1503*, 123−137.
49. Carrell, T. G., Tyryshkin, A. M., and Dismukes, G. C. (2001) *J. Biol. Inorg. Chem. 7*, 2−22.
50. Berthold, D. A., Babcock, G. T., and Yocum, C. F. (1981) *FEBS Lett. 134*, 231−234.
51. Ono, T.-A., and Inoue, Y. (1988) *FEBS Lett. 227*, 147−152.
52. Porra, R. J., Thompson, W. A., and Kriedemann, P. E. (1989) *Biochim. Biophys. Acta 975*, 384−394.
53. Messinger, J., Badger, M., and Wydrzynski, T. (1995) *Proc. Natl. Acad. Sci. U.S.A. 92*, 3209−3213.
54. Hillier, W., Messinger, J., and Wydrzynski, T. (1998) *Biochemistry 37*, 16908−16914.
55. Hillier, W., and Wydrzynski, T. (2000) *Biochemsitry 39*, 4399−4405.
56. Hillier, W. (1999) Ph.D. Thesis, The Australian National University, Canberra, Australia.
57. Shen, J.-R., and Inoue, Y. (1991) *Plant Cell Physiol. 32*, 453−457.
58. Hendry, G. (2003) Ph.D. Thesis, The Australian National University, Canberra, Australia.
59. Hendry, G. S., and Wydrzynski, T. (2002) *Biochemistry 41*, 13328−13334.
60. Hillier, W., Hendry, G., Burnap, R. L., and Wydrzynski, T. (2001) *J. Biol. Chem. 276*, 46917−46924.
61. Hillier, W., and Wydrzynski, T. (2001) *Biochim. Biophys. Acta 1503*, 197−209.
62. Richens, D. T. (1997) in *The Chemistry of Aqua Ions*, John Wiley and Sons, West Sussex, England.
63. Lincoln, S. F., and Merbach, A. E. (1995) *Adv. Inorg. Chem. 42*, 1−88.
64. Westerhausen, M. (1998) *Coord. Chem. Rev. 176*, 157−210.
65. Vander Meulen, K. A., Hobson, A., and Yocum, C. F. (2002) *Biochemistry 41*, 958−966.
66. Riggs-Gelasco, P. J., Mei, R., Ghanotokis, D. F., Yocum, C. F., and Penner-Hahn, J. E. (1996) *J. Am. Chem. Soc. 118*, 2400−2410.

BI034279I